Modeling of a Flexible Manipulator Dynamics Based upon Holzer's Model

Atsushi Konno
Dept. of Mechano-Informatics
University of Tokyo
Tokyo 113, JAPAN

Masaru Uchiyama
Dept. of Aeronautics and Space Engineering
Tohoku University
Sendai 980-77, JAPAN

Abstract

An approach to modeling flexible manipulators consisting of rotary joints and flexible links is proposed in this paper. In the proposed approach, flexible manipulators are modeled by lumped-masses and massless springs on the basis of Holzer's model, which is known as an approximate model for vibration analysis of flexible systems. Due to its simplicity, the constructed model is advantageous to the study of kinematics, dynamics and control strategy of complicated systems such as three dimensional multi-link multi-DOF flexible manipulators. Based on the model, dynamic equations of motion are derived using Lagrange's equation. Kinematics and the relationship between the dynamics of rigid manipulators and flexible manipulators are also discussed. The effectiveness of the model is evaluated by comparing the results of simulation with those of the experiment.

1 Introduction

Conventional design of industrial manipulators has been bulky enough to prevent manipulators from elastic deformation and vibration. Therefore, current industrial manipulators are unable to perform quick movements, and consume superfluous energy merely staying in the same position. For these reasons, lightweight manipulators are expected to be a new technology in industrial applications.

Reduction of weight necessarily induces arm flexibility, and thus control of elastic deformation and vibration is needed. Therefore, a considerable number of studies have been devoted to flexible manipulators over the past few decades.

In the study of flexible manipulators, modeling has been one of the hot research topics. In the beginning, some of the approximate methods for vibration analysis of flexible systems [1] have been applied to modeling of flexible manipulators. For instance, Cannon and Schmitz applied the assumed mode method to the modeling of a one-link flexible manipulator [2], while Book has proposed the recursive Lagrangian dynamics [3]. In [3], deflection of link is obtained using the assumed mode method, and kinematics is discussed using 4×4 transformation matrices. The finite element method has also been applied to a dynamic model of flexible manipulators [4, 5].

The model constructed using assumed mode method is difficult to apply to the complicated system as a three dimensional multi-link multi-DOF flexible manipulator, since determination of the displacement components and the time-varying amplitude of each mode becomes complicated. Needless to say, solving partial differential equations is not useful in cases of complicated systems. As far as finite element method is concerned, it is difficult to obtain the dynamic equations symbolically, and thus, it is not easy to discuss the control strategy, kinematics, and so on.

In order to study the complicated system, some simple models have been proposed over the last few years. However, most of the papers dealt with only two-link planar manipulators (e.g. [6]), or placed emphasis upon the approximation of the elastic link shape [7, 8].

In this paper, an approach of modeling is proposed for flexible manipulators consisting of rotary joints and flexible links. The aim of the paper is similar to the approach of [6, 7, 8], however due to its simplicity, the proposed model is easier for discussing kinematics, controllability, dynamics, control strategy with regard to complicated systems such as three dimensional multi-link multi-DOF flexible manipulators. Simulation based on the proposed model is performed, and the effectiveness of the model is evaluated by comparing the results of simulation with those of experiments.

2 Lumped-masses and spring model

Holzer's method is one of the approximate methods for torsional vibration analysis of flexible shafts, and was extended by Myklestad to the bending vibration analysis of flexible beams [1]. In Holzer's (Myklestad's) method, a flexible structure is modeled as a series of lumped-masses and massless springs. The lumped-masses are called *stations*, while the massless springs are called *fields*. The remarkable difference between flexible structures and flexible manipulators depends on whether they have actuated joints or not, and thus, a flexible manipulator can be regarded, in a sense, as a series of flexible structures connected by actuated joints. Bearing in mind the difference between structures and manipulators, *joints* have been added to the conventional Holzer's method in applying it to the modeling of flexible manipulators.

Proc. IROS 96
0-7803-3213-X/96/ $ 5.00

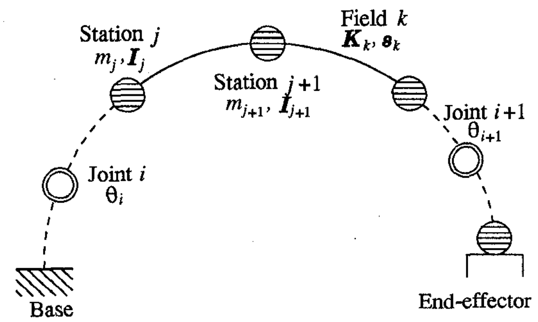

Figure 1: A conceptual sketch of Holzer's modeling of the flexible robot.

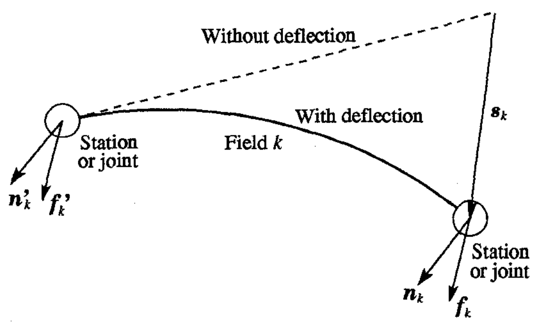

Figure 2: Forces, moments and deflections at the *field k*.

Flexible manipulators consisting of actuated rotary joints and flexible links are considered here. Each flexible link is modeled by a series of *stations* and *fields*. Joint flexibility can also be modeled by *fields* whose length is zero. Each series of *stations* and *fields* is connected by *joints*. Consequently, flexible manipulators are modeled as shown in Figure 1. Important parameters are the joint angle θ_i of the *joint i*, the mass m_j and the inertia tensor $\boldsymbol{I}_j$ of the *station j*, and the spring constant $\boldsymbol{K}_k$ and the deflections $\boldsymbol{s}_k$ of the *field k*. The joint angle vector $\boldsymbol{\theta}$ is defined as

$$\boldsymbol{\theta} = \begin{bmatrix} \theta_1 & \theta_2 & \cdots & \theta_n \end{bmatrix}^T, \tag{1}$$

and the inertia matrix $\boldsymbol{R}_j$ as

$$\boldsymbol{R}_j = \begin{bmatrix} m_j \boldsymbol{E}_3 & \boldsymbol{0} \\ \boldsymbol{0} & \boldsymbol{I}_j \end{bmatrix}, \tag{2}$$

where $\boldsymbol{E}_3$ is the 3×3 unit matrix.

Figure 2 shows the forces and moments at both ends of the *field k* and its deflection due to them. The field deflection vector $\boldsymbol{s}_k$ generally consists of six components: three translational and three rotational deflections. The force $\boldsymbol{f}_k$ and the moment $\boldsymbol{n}_k$ at one end of

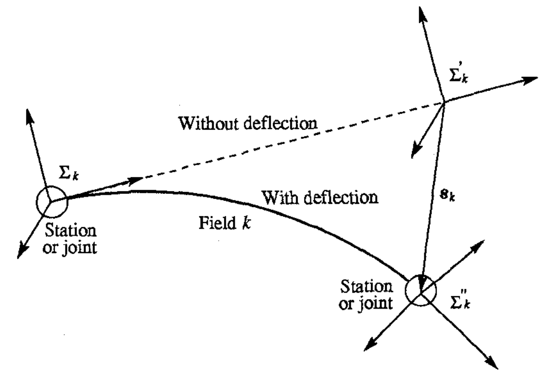

Figure 3: Coordinate systems at the *field k*.

the *field k* is given by

$$\begin{bmatrix} \boldsymbol{f}_k \\ \boldsymbol{n}_k \end{bmatrix} = \boldsymbol{K}_k \boldsymbol{s}_k. \tag{3}$$

The force $\boldsymbol{f}'_k$ and the moment $\boldsymbol{n}'_k$ at the other end can be easily calculated from $\boldsymbol{f}_k$ and $\boldsymbol{n}_k$. The vector $\boldsymbol{e}$ which represents all the components of the field deflections is given by

$$\begin{aligned} \boldsymbol{e} &= \begin{bmatrix} \boldsymbol{s}_1^T & \boldsymbol{s}_2^T & \cdots & \boldsymbol{s}_q^T \end{bmatrix}^T \\ &= \begin{bmatrix} e_1 & e_2 & \cdots & e_m \end{bmatrix}^T. \end{aligned} \tag{4}$$

3 Kinematics

3.1 Transfer matrices

Coordinate system Σ_k is settled at the end on the base side of the *field k*, while Σ''_k is settled at the other end. (see Figure 3).

Transfer matrix relating the coordinate system Σ_k with Σ''_k is represented as $\boldsymbol{F}_k$. $\boldsymbol{F}_k$ is named *field transfer matrix* here. In cases where the field deflection vector $\boldsymbol{s}_k$ consists of three translational and three rotational deflections as

$$\boldsymbol{s}_k = [\delta_x, \delta_y, \delta_z, \phi_x, \phi_y, \phi_z]^T, \tag{5}$$

$\boldsymbol{F}_k$ is represented by 4×4 matrix as

$$\boldsymbol{F}_k = \begin{bmatrix} C_{yk}C_{zk} & -C_{yk}S_{zk} & S_{yk} & L_k + \delta_{xk} \\ S_{xk}S_{yk}C_{zk} + C_{xk}S_{zk} & -S_{xk}S_{yk}S_{zk} + C_{xk}C_{zk} & -S_{xk}C_{yk} & \delta_{yk} \\ -C_{xk}S_{yk}C_{zk} + S_{xk}S_{zk} & C_{xk}S_{yk}S_{zk} + S_{xk}C_{zk} & C_{xk}C_{yk} & \delta_{zk} \\ 0 & 0 & 0 & 1 \end{bmatrix} \tag{6}$$

where L_k is the length of the *field k*, $C_{pk} = \cos\phi_{pk}$, $S_{pk} = \sin\phi_{pk}$ ($p = x$, y and z). If ϕ_{xk}, ϕ_{yk}, ϕ_{zk}, and

δ_{xk} can be assumed to be small, $\boldsymbol{F}_i$ can be represented in a more compact form

$$\boldsymbol{F}_k = \begin{bmatrix} 1 & -\phi_{zk} & \phi_{yk} & L_k \\ \phi_{zk} & 1 & -\phi_{xk} & \delta_{yk} \\ -\phi_{yk} & \phi_{xk} & 1 & \delta_{zk} \\ 0 & 0 & 0 & 1 \end{bmatrix} \quad (7)$$

Transfer matrix $\boldsymbol{S}_j$ relates the coordinate systems on both sides of *station* j, and is named *station transfer matrix* here.

Consequently, transfer matrix $\boldsymbol{L}_i$ relating the coordinate systems on both sides of link i is defined as follows:

$$\boldsymbol{L}_i = \boldsymbol{F}_{i1}\boldsymbol{S}_{i1}\boldsymbol{F}_{i2}\boldsymbol{S}_{i2}\cdots\boldsymbol{S}_{i,f-1}\boldsymbol{F}_{if}, \quad (8)$$

where the link i includes *fields* $i1, \cdots, if$ and *stations* $i1, \cdots, i(f-1)$.

Transfer matrix $\boldsymbol{A}_i$ relates the coordinate systems on both sides of *joint* i, and consequently, $\boldsymbol{A}_i$ is a function of θ_i. Using $\boldsymbol{L}_i$, $\boldsymbol{A}_i$, $\boldsymbol{S}_j$ and $\boldsymbol{F}_k$, transformation from *station* j to the base frame is expressed as follows:

$${}^0\boldsymbol{T}_j = \boldsymbol{L}_0\boldsymbol{A}_1\boldsymbol{L}_1\cdots\boldsymbol{A}_{N_j}\boldsymbol{F}_{N_j'}\boldsymbol{S}_{N_j''}\cdots\boldsymbol{F}_{Q_j}, \quad (9)$$

where N_j and Q_j represent the greatest numbers of the *joint* and *field* which are on the base side of *station* j.

3.2 Velocity and acceleration of station j

In the proposed modeling, the motion of a manipulator, either flexible or rigid, is represented by the motion of all *stations*. Kinematic equations derived here are, therefore, those needed to obtain positions, velocities, and accelerations of each *station*.

Let $\boldsymbol{p}_j$ and $\boldsymbol{\nu}_j$ represent position and velocity vectors of the *station* j, respectively. Each vector has three translational and three rotational components and they are represented by

$$\boldsymbol{p}_j = \begin{bmatrix} \boldsymbol{r}_j^T & \alpha_j & \beta_j & \gamma_j \end{bmatrix}^T, \quad (10)$$

$$\boldsymbol{\nu}_j = \begin{bmatrix} \boldsymbol{v}_j \\ \boldsymbol{\omega}_j \end{bmatrix}, \quad (11)$$

respectively, where $\boldsymbol{r}_j$ represents the position, α_j, β_j and γ_j are the orientation angles, and $\boldsymbol{v}_j$, $\boldsymbol{\omega}_j$ are the translational and rotational velocities of *station* j, respectively.

The velocity $\boldsymbol{\nu}_j$ is computed by the linear equation:

$$\boldsymbol{\nu}_j = \boldsymbol{J}_{\theta j}\dot{\boldsymbol{\theta}} + \boldsymbol{J}_{ej}\dot{\boldsymbol{e}}, \quad (12)$$

where $\boldsymbol{J}_{\theta j}$ and $\boldsymbol{J}_{\theta j}$ are the Jacobian matrices represented by

$$\boldsymbol{J}_{\theta j} = \begin{bmatrix} \boldsymbol{J}_{\theta j}^v \\ \boldsymbol{J}_{\theta j}^\omega \end{bmatrix} = \begin{bmatrix} \boldsymbol{j}_{\theta j1} \ \boldsymbol{j}_{\theta j2} \cdots \boldsymbol{j}_{\theta jN_j} \ \boldsymbol{0} \cdots \boldsymbol{0} \end{bmatrix}, \quad (13)$$

$$\boldsymbol{J}_{ej} = \begin{bmatrix} \boldsymbol{J}_{ej}^v \\ \boldsymbol{J}_{ej}^\omega \end{bmatrix} = \begin{bmatrix} \boldsymbol{j}_{ej1} \ \boldsymbol{j}_{ej2} \cdots \boldsymbol{j}_{ejM_j} \ \boldsymbol{0} \cdots \boldsymbol{0} \end{bmatrix}, \quad (14)$$

where N_j and M_j are the greatest number of the joint and the field deflection variable on the base side of the *station* j. Equation (12) can be more concisely represented as

$$\boldsymbol{\nu}_j = \boldsymbol{J}_j\dot{\boldsymbol{q}}, \quad (15)$$

where

$$\boldsymbol{J}_j = \begin{bmatrix} \boldsymbol{J}_{\theta j} & \boldsymbol{J}_{ej} \end{bmatrix}, \quad (16)$$

$$\dot{\boldsymbol{q}} = \begin{bmatrix} \dot{\boldsymbol{\theta}} \\ \dot{\boldsymbol{e}} \end{bmatrix}. \quad (17)$$

4 Dynamics

Equations of motion are derived using Lagrange's equations. First, the kinetic energy T and the potential energy U of the robot are given by

$$T = \sum_{i=1}^{n}\frac{1}{2}I_{ai}\dot{\theta}_i^2 + \sum_{j=1}^{p}\frac{1}{2}\boldsymbol{\nu}_j^T\boldsymbol{R}_j\boldsymbol{\nu}_j, \quad (18)$$

$$U = \sum_{k=1}^{q}\frac{1}{2}\boldsymbol{s}_k^T\boldsymbol{K}_k\boldsymbol{s}_k - \sum_{j=1}^{p}\boldsymbol{r}_j^T m_j\boldsymbol{g} = \frac{1}{2}\boldsymbol{e}^T\boldsymbol{K}\boldsymbol{e} - \sum_{j=1}^{p}\boldsymbol{r}_j^T m_j\boldsymbol{g}, \quad (19)$$

respectively, where

$$\boldsymbol{K} = \begin{bmatrix} \boldsymbol{K}_1 & & \boldsymbol{0} \\ & \ddots & \\ \boldsymbol{0} & & \boldsymbol{K}_q \end{bmatrix}, \quad (20)$$

the vector $\boldsymbol{g}$ represents the acceleration of gravity, I_{ai} is the moment of inertia of the i-th motor rotor, and p, q are the numbers of *stations* and *fields*, respectively. The kinetic energy of the motor rotor is approximated by the one for the motor which does not change its position or orientation. The Lagrangian is computed using T and U as follows:

$$L = T - U = \sum_{i=1}^{n}\frac{1}{2}I_{ai}\dot{\theta}_i^2 + \sum_{j=1}^{p}\left(\frac{1}{2}\boldsymbol{\nu}_j^T\boldsymbol{R}_j\boldsymbol{\nu}_j + \boldsymbol{r}_j^T m_j\boldsymbol{g}\right) - \frac{1}{2}\boldsymbol{e}^T\boldsymbol{K}\boldsymbol{e}. \quad (21)$$

The Lagrange's equations are given by

$$\tau_i = \frac{d}{dt}\left(\frac{\partial L}{\partial\dot{\theta}_i}\right) - \frac{\partial L}{\partial\theta_i} \quad (i = 1,\ 2,\ \cdots,\ n), \quad (22)$$

$$0 = \frac{d}{dt}\left(\frac{\partial L}{\partial\dot{e}_l}\right) - \frac{\partial L}{\partial e_l} \quad (l = 1,\ 2,\ \cdots,\ m). \quad (23)$$

The first equation and the second equation are named as the equation of link motion and the equation of field motion, respectively. The first equation represents the rigid motion of the links and the second the elastic motion of the *fields*, that is, the link vibration.

4.1 Equation of link motion

Substituting Eq. (21) into (22) and bearing in mind Eq. (15), each term of Eq. (22) is respectively represented as

$$\frac{d}{dt}\left(\frac{\partial L}{\partial \dot{\theta}_i}\right) = I_{ai}\ddot{\theta}_i + \sum_{j=P_i^\theta}^{p}\left(\boldsymbol{j}_{\theta ji}^T \boldsymbol{R}_j \boldsymbol{J}_j\right)\ddot{\boldsymbol{q}} + \sum_{j=P_i^\theta}^{p}\frac{d}{dt}\left(\boldsymbol{j}_{\theta ji}^T \boldsymbol{R}_j \boldsymbol{J}_j\right)\dot{\boldsymbol{q}}, \tag{24}$$

$$\frac{\partial L}{\partial \theta_i} = \frac{1}{2}\frac{\partial}{\partial \theta_i}\sum_{j=P_i^\theta}^{p}\left(\dot{\boldsymbol{q}}^T \boldsymbol{J}_j^T \boldsymbol{R}_j \boldsymbol{J}_j \dot{\boldsymbol{q}}\right) + \sum_{j=P_i^\theta}^{p}\frac{\partial \boldsymbol{r}_j^T}{\partial \theta_i} m_j \boldsymbol{g}, \tag{25}$$

where P_i^θ is the smallest number of the station which is on the end-effector side of *joint i*. If $\boldsymbol{j}_{\theta ji}$ and $\boldsymbol{g}_6$ are defined by

$$\boldsymbol{j}_{\theta ji} = \begin{bmatrix} \boldsymbol{j}_{\theta ji}^v \\ \boldsymbol{j}_{\theta ji}^\omega \end{bmatrix}, \tag{26}$$

$$\boldsymbol{g}_6 = \begin{bmatrix} \boldsymbol{g} \\ \boldsymbol{0}_{3\times 1} \end{bmatrix}, \tag{27}$$

respectively, then

$$\frac{\partial \boldsymbol{r}_j^T}{\partial \theta_i} m_j \boldsymbol{g} = \boldsymbol{j}_{\theta ji}^T m_j \boldsymbol{g}_6 \tag{28}$$

is obtained. Substituting Eqs. (24), (25) and (28) into Eq. (22),

$$\begin{aligned}\tau_i = {} & I_{ai}\ddot{\theta}_i + \sum_{j=P_i^\theta}^{p}\left(\boldsymbol{j}_{\theta ji}^T \boldsymbol{R}_j \boldsymbol{J}_j\right)\ddot{\boldsymbol{q}} + \sum_{j=P_i^\theta}^{p}\frac{d}{dt}\left(\boldsymbol{j}_{\theta ji}^T \boldsymbol{R}_j \boldsymbol{J}_j\right)\dot{\boldsymbol{q}} \\ & -\frac{1}{2}\frac{\partial}{\partial \theta_i}\sum_{j=P_i^\theta}^{p}\left(\dot{\boldsymbol{q}}^T \boldsymbol{J}_j^T \boldsymbol{R}_j \boldsymbol{J}_j \dot{\boldsymbol{q}}\right) - \sum_{j=P_i^\theta}^{p}\left(\boldsymbol{j}_{\theta ji}^T m_j \boldsymbol{g}_6\right)\end{aligned} \tag{29}$$

is obtained. Finally, the equation of link motion is obtained as follows:

$$\begin{aligned}\boldsymbol{\tau} = {} & \boldsymbol{R}_a\ddot{\boldsymbol{\theta}} + \left(\sum_{j=1}^{p}\boldsymbol{J}_{\theta j}^T \boldsymbol{R}_j \boldsymbol{J}_{\theta j}\right)\ddot{\boldsymbol{\theta}} + \left(\sum_{j=1}^{p}\boldsymbol{J}_{\theta j}^T \boldsymbol{R}_j \boldsymbol{J}_{ej}\right)\ddot{\boldsymbol{e}} \\ & + \frac{d}{dt}\left(\sum_{j=1}^{p}\boldsymbol{J}_{\theta j}^T \boldsymbol{R}_j \boldsymbol{J}_j\right)\dot{\boldsymbol{q}} - \frac{1}{2}\frac{\partial}{\partial \boldsymbol{\theta}}\sum_{j=1}^{p}\left(\dot{\boldsymbol{q}}^T \boldsymbol{J}_j^T \boldsymbol{R}_j \boldsymbol{J}_j \dot{\boldsymbol{q}}\right) \\ & - \sum_{j=1}^{p}\left(\boldsymbol{J}_{\theta j}^T m_j \boldsymbol{g}_6\right),\end{aligned} \tag{30}$$

where

$$\boldsymbol{R}_a = \begin{bmatrix} I_{a1} & & \boldsymbol{0} \\ & \ddots & \\ \boldsymbol{0} & & I_{an} \end{bmatrix}, \tag{31}$$

or in a more compact form:

$$\boldsymbol{\tau} = \boldsymbol{M}_{11}(\boldsymbol{\theta}, \boldsymbol{e})\ddot{\boldsymbol{\theta}} + \boldsymbol{M}_{12}(\boldsymbol{\theta}, \boldsymbol{e})\ddot{\boldsymbol{e}} + \boldsymbol{h}_1(\boldsymbol{\theta}, \dot{\boldsymbol{\theta}}, \boldsymbol{e}, \dot{\boldsymbol{e}}) + \boldsymbol{g}_1(\boldsymbol{\theta}, \boldsymbol{e}). \tag{32}$$

4.2 Equation of field motion

Substituting Eq. (21) into (23) and bearing in mind Eq. (15), each term of Eq. (23) is respectively represented as

$$\frac{d}{dt}\left(\frac{\partial L}{\partial \dot{e}_l}\right) = \sum_{j=P_l^e}^{p}\left(\boldsymbol{j}_{ejl}^T \boldsymbol{R}_j \boldsymbol{J}_j\right)\ddot{\boldsymbol{q}} + \sum_{j=P_l^e}^{p}\frac{d}{dt}\left(\boldsymbol{j}_{ejl}^T \boldsymbol{R}_j \boldsymbol{J}_j\right)\dot{\boldsymbol{q}} \tag{33}$$

$$\begin{aligned}\frac{\partial L}{\partial e_l} = {} & \frac{1}{2}\frac{\partial}{\partial e_l}\sum_{j=P_l^e}^{p}\left(\dot{\boldsymbol{q}}^T \boldsymbol{J}_j^T \boldsymbol{R}_j \boldsymbol{J}_j \dot{\boldsymbol{q}}\right) + \sum_{j=P_l^e}^{p}\frac{\partial \boldsymbol{r}_j^T}{\partial e_l} m_j \boldsymbol{g} \\ & - \frac{\partial \boldsymbol{e}^T}{\partial e_l}\boldsymbol{K}\boldsymbol{e}\end{aligned} \tag{34}$$

where P_l^e is the smallest number of the station which is on the end-effector side of the *field* having the deflection variable e_l. If $\boldsymbol{j}_{eji}$ is defined by

$$\boldsymbol{j}_{ejl} = \begin{bmatrix} \boldsymbol{j}_{ejl}^v \\ \boldsymbol{j}_{ejl}^\omega \end{bmatrix}, \tag{35}$$

then

$$\frac{\partial \boldsymbol{r}_j^T}{\partial e_l} m_j \boldsymbol{g} = \boldsymbol{j}_{ejl}^T m_j \boldsymbol{g}_6 \tag{36}$$

is obtained. Substituting Eqs. (33), (34) and (36) into Eq. (23),

$$\begin{aligned}0 = {} & \sum_{j=P_l^e}^{p}\left(\boldsymbol{j}_{ejl}^T \boldsymbol{R}_j \boldsymbol{J}_j\right)\ddot{\boldsymbol{q}} + \sum_{j=P_l^e}^{p}\frac{d}{dt}\left(\boldsymbol{j}_{ejl}^T \boldsymbol{R}_j \boldsymbol{J}_j\right)\dot{\boldsymbol{q}} \\ & -\frac{1}{2}\frac{\partial}{\partial e_l}\sum_{j=P_l^e}^{p}\left(\dot{\boldsymbol{q}}_j^T \boldsymbol{J}_j^T \boldsymbol{R}_j \boldsymbol{J}_j \dot{\boldsymbol{q}}_j\right) - \sum_{j=P_l^e}^{p}\left(\boldsymbol{j}_{ejl}^T m_j \boldsymbol{g}_6\right) \\ & + \frac{\partial \boldsymbol{e}^T}{\partial e_l}\boldsymbol{K}\boldsymbol{e}\end{aligned} \tag{37}$$

is obtained. Finally, equation of field motion is obtained as follows:

$$\begin{aligned}\boldsymbol{0} = {} & \left(\sum_{j=1}^{p}\boldsymbol{J}_{ej}^T \boldsymbol{R}_j \boldsymbol{J}_{\theta j}\right)\ddot{\boldsymbol{\theta}} + \left(\sum_{j=1}^{p}\boldsymbol{J}_{ej}^T \boldsymbol{R}_j \boldsymbol{J}_{ej}\right)\ddot{\boldsymbol{e}} \\ & + \frac{d}{dt}\left(\sum_{j=1}^{p}\boldsymbol{J}_{ej}^T \boldsymbol{R}_j \boldsymbol{J}_j\right)\dot{\boldsymbol{q}} - \frac{1}{2}\frac{\partial}{\partial \boldsymbol{e}}\sum_{j=1}^{p}\left(\dot{\boldsymbol{q}}^T \boldsymbol{J}_j^T \boldsymbol{R}_j \boldsymbol{J}_j \dot{\boldsymbol{q}}\right) \\ & - \sum_{j=1}^{p}\left(\boldsymbol{J}_{ej}^T m_j \boldsymbol{g}_6\right) + \boldsymbol{K}\boldsymbol{e},\end{aligned} \tag{38}$$

or in a more compact form:

$$\begin{aligned}\boldsymbol{0} = {} & \boldsymbol{M}_{21}(\boldsymbol{\theta}, \boldsymbol{e})\ddot{\boldsymbol{\theta}} + \boldsymbol{M}_{22}(\boldsymbol{\theta}, \boldsymbol{e})\ddot{\boldsymbol{e}} + \boldsymbol{h}_2(\boldsymbol{\theta}, \dot{\boldsymbol{\theta}}, \boldsymbol{e}, \dot{\boldsymbol{e}}) \\ & + \boldsymbol{g}_2(\boldsymbol{\theta}, \boldsymbol{e}) + \boldsymbol{K}\boldsymbol{e}\end{aligned} \tag{39}$$

5 Relation with rigid manipulators' dynamics

It has been shown that the motion of flexible manipulators is expressed by the equation of link motion and the equation of field motion. The relation between these equations and the equations of motion of rigid manipulators is discussed in this section.

Substituting $\ddot{\boldsymbol{e}} = \dot{\boldsymbol{e}} = \boldsymbol{e} = \boldsymbol{0}$ into eq. (30),

$$\begin{aligned}\boldsymbol{\tau} &= \boldsymbol{R}_a\ddot{\boldsymbol{\theta}} + \left(\sum_{j=1}^{p} \boldsymbol{J}_{\theta j}^T \boldsymbol{R}_j \boldsymbol{J}_{\theta j}\right)\ddot{\boldsymbol{\theta}} \\ &+ \frac{d}{dt}\left(\sum_{j=1}^{p} \boldsymbol{J}_{\theta j}^T \boldsymbol{R}_j \boldsymbol{J}_{\theta j}\right)\dot{\boldsymbol{\theta}} \\ &- \frac{1}{2}\frac{\partial}{\partial \boldsymbol{\theta}}\sum_{j=1}^{p}\left(\dot{\boldsymbol{\theta}}^T \boldsymbol{J}_{\theta j}^T \boldsymbol{R}_j \boldsymbol{J}_{\theta j}\dot{\boldsymbol{\theta}}\right) - \sum_{j=1}^{p}\left(\boldsymbol{J}_{\theta j}^T m_j \boldsymbol{g}_6\right)\end{aligned} \tag{40}$$

is obtained. Equation (40) represents the motion of rigid manipulators. It means that the motion of both rigid and flexible manipulators is represented by the same equation, i.e., equation of link motion (30).

In the case of $\ddot{\boldsymbol{e}} = \dot{\boldsymbol{e}} = \boldsymbol{e} = \boldsymbol{0}$, considering Eq. (3), the equation of field motion becomes as follows:

$$\begin{aligned}\boldsymbol{0} &= \left(\sum_{j=1}^{p} \boldsymbol{J}_{ej}^T \boldsymbol{R}_j \boldsymbol{J}_{\theta j}\right)\ddot{\boldsymbol{\theta}} + \frac{d}{dt}\left(\sum_{j=1}^{p} \boldsymbol{J}_{ej}^T \boldsymbol{R}_j \boldsymbol{J}_{\theta j}\right)\dot{\boldsymbol{\theta}} \\ &- \frac{1}{2}\frac{\partial}{\partial \boldsymbol{e}}\sum_{j=1}^{p}\left(\dot{\boldsymbol{\theta}}^T \boldsymbol{J}_{\theta j}^T \boldsymbol{R}_j \boldsymbol{J}_{\theta j}\dot{\boldsymbol{\theta}}\right) - \sum_{j=1}^{p}\left(\boldsymbol{J}_{ej}^T m_j \boldsymbol{g}_6\right) \\ &+ \begin{bmatrix} \boldsymbol{f}_1 \\ \boldsymbol{n}_1 \\ \vdots \\ \boldsymbol{f}_q \\ \boldsymbol{n}_q \end{bmatrix}.\end{aligned} \tag{41}$$

From Eq. (41), forces and moments generated at each *field* are obtained.

As a result of the above discussion, a rigid manipulator can be considered as a sort of variation of flexible manipulators.

6 A case study

The modeling method proposed in this paper is applied to an experimental flexible manipulator called ADAM (Figure 4), which has two elastic links and seven joints in both left and right arms. The validity of the modeling is evaluated by comparing results of simulation based on the model with experimental results. For simplicity, moment of inertia generated at stations is not considered here.

Simplified equations of motion without considering the moment of inertia at stations are:

$$\begin{aligned}\boldsymbol{\tau} &= \boldsymbol{R}_a\ddot{\boldsymbol{\theta}} + \left(\sum_{j=1}^{p} m_j \boldsymbol{J}_{\theta j}^{vT} \boldsymbol{J}_{\theta j}^v\right)\ddot{\boldsymbol{\theta}} + \left(\sum_{j=1}^{p} m_j \boldsymbol{J}_{\theta j}^{vT} \boldsymbol{J}_{ej}^v\right)\ddot{\boldsymbol{e}} \\ &+ \frac{d}{dt}\left(\sum_{j=1}^{p} m_j \boldsymbol{J}_{\theta j}^{vT} \boldsymbol{J}_j^v\right)\dot{\boldsymbol{q}} - \frac{1}{2}\frac{\partial}{\partial \boldsymbol{\theta}}\sum_{j=1}^{p} m_j\left(\dot{\boldsymbol{q}}^T \boldsymbol{J}_j^{vT} \boldsymbol{J}_j^v \dot{\boldsymbol{q}}\right) \\ &- \sum_{j=1}^{p}\left(\boldsymbol{J}_{\theta j}^{vT} m_j \boldsymbol{g}\right)\end{aligned} \tag{42}$$

$$\begin{aligned}\boldsymbol{0} &= \left(\sum_{j=1}^{p} m_j \boldsymbol{J}_{ej}^{vT} \boldsymbol{J}_{\theta j}^v\right)\ddot{\boldsymbol{\theta}} + \left(\sum_{j=1}^{p} m_j \boldsymbol{J}_{ej}^{vT} \boldsymbol{J}_{ej}^v\right)\ddot{\boldsymbol{e}} \\ &+ \frac{d}{dt}\left(\sum_{j=1}^{p} m_j \boldsymbol{J}_{ej}^{vT} \boldsymbol{J}_j^v\right)\dot{\boldsymbol{q}} - \frac{1}{2}\frac{\partial}{\partial \boldsymbol{e}}\sum_{j=1}^{p} m_j\left(\dot{\boldsymbol{q}}^T \boldsymbol{J}_j^{vT} \boldsymbol{J}_j^v \dot{\boldsymbol{q}}\right) \\ &- \sum_{j=1}^{p}\left(\boldsymbol{J}_{ej}^{vT} m_j \boldsymbol{g}\right) + \boldsymbol{K}\boldsymbol{e}.\end{aligned} \tag{43}$$

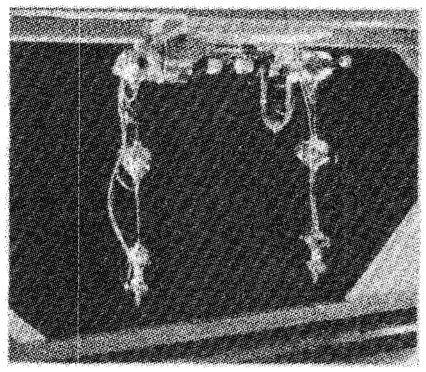

Figure 4: Overview of the experimental manipulator ADAM.

Simulator is programmed based on the Eqs. (42) and (43).

6.1 Modeling of flexible manipulator ADAM

The model of the experimental flexible manipulator ADAM is constructed as shown in Figure 5. Joints and stations circled by dotted line are placed at the same point. For convenience, *fields* 1, 2, 4 are settled between Joint 1 and Station 1, between Joint 2 and Joint 3, and between Joint 4 and Joint 5, respectively, and they are settled to have no length and no deflection.

The experimental manipulator ADAM has seven joints, however, only four of them (joints 1–4) affect the positioning of end-effector, and thus, joint angle and torque vector are defined as follows:

$$\boldsymbol{\tau} = \begin{bmatrix} \tau_1 & \tau_2 & \tau_3 & \tau_4 \end{bmatrix}^T \tag{44}$$

$$\boldsymbol{\theta} = \begin{bmatrix} \theta_1 & \theta_2 & \theta_3 & \theta_4 \end{bmatrix}^T. \tag{45}$$

Deflection variable vector is defined as

$$\boldsymbol{e} = \begin{bmatrix} \delta_{y3} & \delta_{z3} & \delta_{y5} & \delta_{z5} \end{bmatrix}^T \tag{46}$$

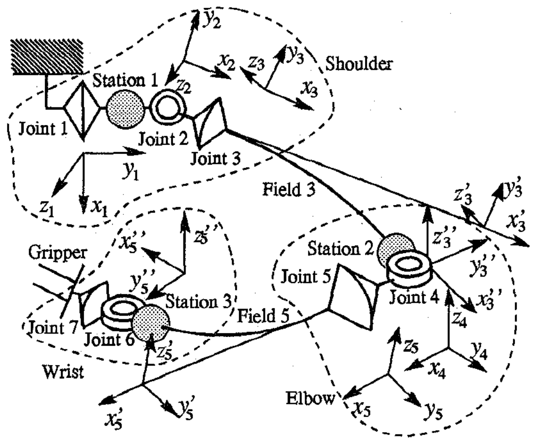

Figure 5: Model of the experimental manipulator ADAM.

where δ_{y3}, δ_{z3}, δ_{y5} and δ_{z5} are the elastic deflections along the y and z axes of field 3 and 5, respectively. The field's torsional deflections can also be considered as a part of $\boldsymbol{e}$, however, since moments of inertia of stations are not considered here, they depend upon bending deflections [9]. Furthermore, deflections along the x axis δ_{x2} and δ_{x3} are assumed to be quite small, and thus, they are not considered here.

Based on the constructed model shown in Figure 5, equations of motion (42) and (43) are computed. Some mechanical parameters of ADAM used in computation of the equations are presented in Table 1.

6.2 Simulation and experiment

Experimental manipulator ADAM has a hardware velocity servo card in the controller, and thus, the velocity servo is programmed in the simulator. The applied torque $\boldsymbol{\tau}$ is assumed to be produced by velocity command $\boldsymbol{V}_{ref}$ and velocity servo as follows:

$$\boldsymbol{\tau} = \boldsymbol{G}_r \boldsymbol{K}_{sp}(\boldsymbol{V}_{ref} - \boldsymbol{K}_{sv}\dot{\boldsymbol{\theta}}_m) \tag{47}$$

where $\boldsymbol{\tau}$ is an applied torque vector, $\dot{\boldsymbol{\theta}}_m$ (rad/s) is the motor rotary velocity vector, $\boldsymbol{V}_{ref}$ (V) is the reference velocity command vector to the robot controller, $\boldsymbol{K}_{sp}$ (Nm/V), $\boldsymbol{K}_{sv}$ (Vs/rad) and $\boldsymbol{G}_r$ are diagonal matrices whose diagonal elements are the velocity servo gain, the voltage/velocity conversion coefficients of the sensors for velocity feedback in the servo and the reduction gear ratios, respectively.

The simulator uses the fourth order Runge-Kutta-Gill formulas to integrate the system of differential equations. Step size of integration is settled as 0.1 (ms). Velocity servo Eq. (47) is assumed to be performed in each 1 (ms), while the sampling period of the control system is assumed to be 10 (ms) which is the same period used in experiments.

Experiment and simulation are performed. Step responses in simulation and experiment for reference position are plotted in Figures 6 and 7, respectively.

Table 1: Parameters in the equations of motion.

Parameter	Notation	Value
Length of fields	l_3 (m)	0.50
	l_5 (m)	0.50
Bending stiffness of fields	E_3I_3 (Nm^2)	291.6
	E_5I_5 (Nm^2)	102.1
Mass of stations	m_2 (kg)	6.6
	m_3 (kg)	3.0
Rotor's inertia	I_{m1} (Nms^2)	1.63×10^{-4}
	I_{m2} (Nms^2)	0.99×10^{-4}
	I_{m3} (Nms^2)	0.99×10^{-4}
	I_{m4} (Nms^2)	0.15×10^{-4}

Position feedback gain is settled as 4.0 (s^{-1}) both in the simulator and the experiment.

In order for the model to be evaluated, the first mode vibration frequencies are taken as characteristic data. As for the vibration which is related to δ_{y3} and δ_{y5}, the vibration frequencies in the simulation and experiment are obtained as 2.865 (Hz) and 2.849 (Hz), respectively. As for the vibration related to δ_{z3} and δ_{z5}, the vibration frequencies in the simulation and experiment are obtained as 2.866 (Hz) and 2.950 (Hz), respectively. Consequently, it is shown that although the constructed model is simple, the motion of the experimental manipulator is well simulated.

7 Conclusion

Holzer's model, which is known as one of the approximate models for torsional vibration problem of flexible structure, is applied to the modeling of flexible manipulator, and based on the model, equations of motion of flexible manipulator are derived. Motion of flexible manipulator is expressed by two equations of motion: one is the equation of link motion, while the other is the equation of field motion. Although these two equations can be derived using other modeling methods, the simple structure of the proposed model is effective to study kinematics, dynamics, and other problems of flexible manipulators. The relation between the rigid manipulator dynamics and the flexible manipulator dynamics is also discussed.

The proposed method has already been applied to the vibration suppression control [10] and study on the vibration controllability [11], and confirmed to be effective to discuss such problems. It is expected that the model will be applied to study on other problems of flexible manipulators, for instance inverse kinematics, inverse dynamics, singularity [12].

References

[1] L. Meirovitch. *Analytical Methods in Vibrations.* Macmillan Publishing Co., Inc., 1967.

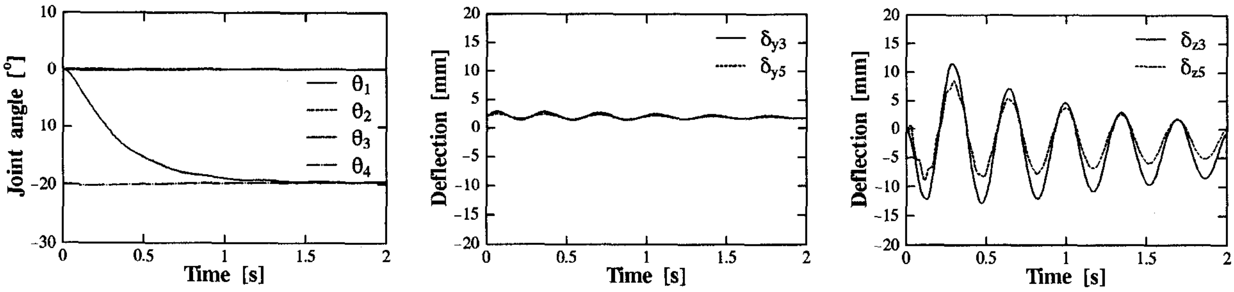

(a) Joint responses. (b) Tip displacement in the y direction. (c) Tip displacement in the z direction.

Figure 6: Simulation results.

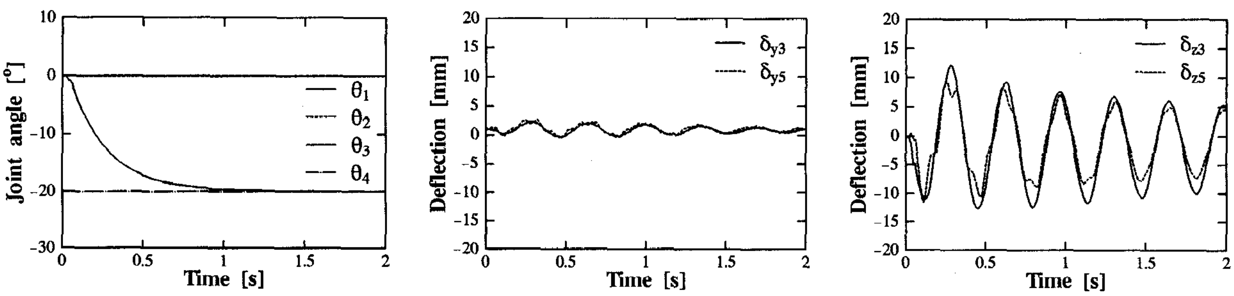

(a) Joint responses. (b) Tip displacement in the y direction. (c) Tip displacement in the z direction.

Figure 7: Experimental results.

[2] R. H. Cannon, Jr. and E. Schmitz. Initial Experiments on the End-Point Control of a Flexible One-Link Robot. *Int. J. of Robotics Research*, Vol. 3, No. 3, pp. 62–75, 1984.

[3] W. J. Book. Recursive Lagrangian Dynamics of Flexible Manipulator Arms. *Int. J. of Robotics Research*, Vol. 3, No. 3, pp. 87–101, 1984.

[4] W. H. Sunada and S. Dubowsky. On the Dynamic Analysis and Behavior of Industrial Robotic Manipulators With Elastic Members. *Trans. of ASME, J. of Mechanisms, Transmissions, and Automation in Design*, Vol. 105, pp. 42–51, 1983.

[5] E. Bayo. A Finite-Element Approach to Control the End-Point Motion of a Single-Link Flexible Robot. *J. of Robotic Systems*, Vol. 4, No. 1, pp. 63–75, 1987.

[6] R. P. Judd and D. R. Falkenburg. Dynamics of Nonrigid Articulated Robot Linkages. *IEEE Trans. on Automatic Control*, Vol. 30, No. 5, pp. 499–502, 1985.

[7] Y. Huang and C. S. G. Lee. Generalization of Newton-Euler Formulation of Dynamic Equations to Nonrigid Manipulators. *Trans. of ASME, J. of Dynamic Systems, Measurement and Control*, Vol. 110, pp. 308–315, 1988.

[8] T. Yoshikawa and K. Hosoda. Modeling of Flexible Manipulators Using Virtual Rigid Links and Passive Joints. In *Proc. of IEEE/RSJ Int. Workshop on Intelligent Robots and Systems IROS '91*, pp. 967–972, Osaka, Japan, November 1991.

[9] T. Yoshikawa, H. Murakami, and K. Hosoda. Modeling and Control of a Three Degree of Freedom Manipulator with Two Flexible Links. In *Proc. of the 29th Conf. on Decision and Control*, pp. 2532–2537, Honolulu, USA, December 1990.

[10] A. Konno and M. Uchiyama. VIBRATION SUPPRESSION CONTROL OF SPATIAL FLEXIBLE MANIPULATOR. *Control Engineering Practice, A Journal of IFAC*, Vol. 3, No. 9, pp. 1315–1321, 1995.

[11] A. Konno, M. Uchiyama, Y. Kito, and M. Murakami. Vibration Controllability of Flexible Manipulators. In *Proc. of IEEE Int. Conf. on Robotics and Automation*, pp. 308–314, San Diego, USA, 1994.

[12] M. Uchiyama and Z.-H. Jiang. Compensability of End-Effector Position Errors for Flexible Robot Manipulators. In *Proc. of 1991 American Control Conference*, pp. 1873–1878, Boston, USA, June 1991.